# UNCLASSIFIED

| AD NUMBER |
|---|
| AD004780 |

| CLASSIFICATION CHANGES |
|---|

TO:       **unclassified**

FROM:      **confidential**

| LIMITATION CHANGES |
|---|

TO:

Approved for public release, distribution unlimited

FROM:

Distribution authorized to U.S. Gov't. agencies and their contractors; Foreign Government Information; JAN 1953. Other requests shall be referred to British Embassy, 3100 Massachusetts Avenue, NW, Washington, DC 20008.

| AUTHORITY |
|---|

DSTL, AVIA 6/23506, 14 Apr 2009; DSTL, AVIA 6/23506, 14 Apr 2009

# THIS PAGE IS UNCLASSIFIED

AD NO 4780
ASTIA FILE COPY

CONFIDENTIAL

# ROYAL AIRCRAFT ESTABLISHMENT

F A R N B O R O U G H ,   H A N T S

TECHNICAL NOTE No: AERO.2220

## THE STUDY OF STABILITY AT
## TRANSONIC SPEEDS BY FREE FLYING MODELS:
# TESTS ON TAILLESS AEROPLANE
# WITH 45° DELTA WING (E27/46)

by

T. LAWRENCE and R. HARMER

CONFIDENTIAL
SECURITY INFORMATION

U.D.C. No. 533.652.5.011.35 : 533.6.013.422/423 : 533.69.043.2 : 533.6.013.13 : 533.6.013.417 (42) E 27/46

ROYAL AIRCRAFT ESTABLISHMENT, FARNBOROUGH

The study of stability at transonic speeds by free flying models.

Tests on a tailless aeroplane with 45° delta wing (E27/46)

by

T. Lawrence
and
R. Harmer

SUMMARY

Five models of a tailless layout having a cropped 45° delta wing (the Boulton Paul Delta layout - E27/46), in which the short period oscillation was excited by small disturbing rockets, were flown in the range 0.8 < M < 1.4. From measurements of the frequency and damping of the oscillations, the variations with Mach number of lift curve slope, aerodynamic centre position and pitching damping have been deduced, and are compared with measurements from other sources.

- 1 -

## LIST OF CONTENTS

## LIST OF TABLES

## LIST OF ILLUSTRATIONS

# SECURITY INFORMATION

## 1. Introduction

Towards the end of 1950, considerable interest was aroused locally in the possibility that some of the planforms being considered for transonic and supersonic flight might, in the tailless layout at transonic speeds, exhibit negative damping of the longitudinal pitching mode. A concentrated theoretical and experimental attack has since been made on the problem, and the present note describes the work done on the Boulton Paul Delta layout [E27/46 - a 45° delta cropped to a taper ratio of 0.125] using the free flight model technique.

## 2. Theory of the Experiment

The philosophy behind an experiment based on a study of the short period longitudinal motion of a free flying model has been discussed at length in Ref.1. For analysis purposes we assume, during any oscillation, that the model is flying at constant speed in a constant atmosphere at constant mean $C_L$, and that the derivatives are constant and linear. The natural frequency of the short period oscillation can then be written (Ref.1, Eqn.9)

$$\omega_n = \frac{1}{\hat{t}}\left[ z_w \frac{m_q}{i_B} - \mu \frac{m_w}{i_B}\right]^{\frac{1}{2}}.$$

Now, especially for tailless layouts, $z_w m_q \ll \mu m_w$, whence

$$\left[\omega_n \hat{t}\right]^2 = -\mu \frac{m_w}{i_B}$$

and thus

$$2\mu i_B \bar{\omega}_n^2 = a_1 H_m$$

where

$$\hat{t} = \mu \frac{\bar{c}}{V}$$

$$\bar{\omega}_n = \omega_n \frac{\bar{c}}{V}$$

$$a_1 = \frac{dC_L}{d\alpha}$$

and $H_m$ = manoeuvre margin

$$= -\left[\frac{dC_m}{dC_L} + h\right] \text{ approx.}$$

Thus from tests on two models with different C.G. positions, it should be possible to determine both the lift curve slope and the manoeuvre margin, and hence the aerodynamic centre position.

Direct measurement of angle-of-attack on the model allows an immediate determination of lift curve slope $a_1$, and hence the same information as before can be obtained from one model. An angle-of-attack meter has been developed and is now in production, but it was not available when the

present experiments were made. However Voepel has shown[2] that the lift curve slope can be computed from comparison of the records of two longitudinally displaced accelerometers. We can write[2]

$$\frac{dn}{d\alpha} = -\frac{V\omega_n}{g}\left[1 - 2\frac{V}{\omega_n d}\left\{\cos\delta - \frac{1}{R}\cos(\delta - \varphi_d)\right\}\right.$$

$$\left. + \frac{V^2}{\omega_n^2 d^2}\left\{1 - \frac{2}{R}\cos\varphi_d + \frac{1}{R^2}\right\}\right]^{-\frac{1}{2}}$$

where $R$ is the scale ratio between two accelerometers displaced by a distance $d$, and $\varphi_d$ is the phase difference between their readings. It will be seen below that we were unable to measure $\varphi_d$ with sufficient accuracy, and it was computed from the relation

$$\sin(\varphi_d + 2\delta) = R\left(\sin 2\delta - \frac{d\omega}{V}\right).$$

It can be shown (Ref.2, Eqn.5) that

$$z_w = \frac{dn}{d\alpha}\cdot\frac{g\hat{t}}{V},$$

and we have used the approximation

$$z_w = -\frac{1}{2}[a_1 + C_D]$$

$$\approx -\frac{1}{2}a_1.$$

The orthodox approach to the longitudinal stability equations gives, for the damping of the short period oscillation [see for example Ref.1, Eqns. 10 and 13]

$$2\lambda\hat{t} = -z_w - \frac{m_{\dot\vartheta}}{i_B}$$

whence
$$-m_{\dot\vartheta} = 2\lambda\hat{t}\,i_B - \frac{1}{2}a_1 i_B.$$

$m_{\dot\vartheta} = m_q + m_{\dot w}$ is in fact what is measured in a tunnel measurement of the damping [see for example Ref.3]. Furthermore, it should be noted that the motion of an actual aeroplane is damped by a combination of pitching ($m_{\dot\vartheta}$) and plunging ($z_w$) modes, whose relative importance is governed by the pitching inertia ($i_B$). It is thus important in the model experiment that the inertia be not too far away from the aeroplane value, if in the limiting cases the significance of the pitching and plunging modes are to be correctly assessed. This point is discussed later.

If $h$ be the position of the axis of rotation on the mean chord, then $m_{\dot\vartheta}$ is a quadratic function of $h$, and we can, following Warren[4] write

$$m_{\dot{\vartheta}} = m_{\dot{\vartheta}_0} + (H - h)^2 z_w$$

where $m_{\dot{\vartheta}_0}$ is the maximum value of $m_{\dot{\vartheta}}$ and occurs when $h = H$.[*] The free flight damping measurements are made at a different axis position for each model (corresponding to different C.G. positions) and before they can be compared the values of $m_{\dot{\vartheta}}$ must be corrected to the same axis position. At first sight it would seem reasonable to reduce the results to show the variation of $m_{\dot{\vartheta}_0}$ and H with Mach number. However H varies significantly from subsonic to supersonic, and since in the aeroplane case the value of h is fixed for all speeds, we have elected to correct the experimental values to a constant value of h. We have chosen $h = 0.556 c_0$, since this is the axis position at which most NPL work has been done; in passing it should be noted that this is aft of the low speed aerodynamic centre, i.e. it is unreal for an aeroplane.

In practice the damping results showed considerable scatter, and the calculation of $m_{\dot{\vartheta}_0}$ and H from results at two C.G. positions was not possible. Between $0.7 < M < 0.93$ we have used NPL results on models with two axis positions[5] to calculate H, and for $1.15 < M < 1.4$ we have used Ref.4. The details are further discussed below.

## 3    Experimental Method

The experimental technique was developed concurrently with the present experiments, which suffer in consequence. Tests were made on 5 models having three different "fuselages", but all models had the correct gross planform of 10% RAE 102 section; all 5 tests are reported here because it is believed the results obtained are relevant.

The experimental method was to study the short period longitudinal motion of a free flying model; in particular, to study the frequency and damping of the motion, as displayed by accelerometers mounted on, and longitudinally displaced from, the C.G. of the model.

The fuselage of the model took one of 3 forms:-

(a) Originally, on Model 1, the fuselage was a simple cylindrical body 5 inches diameter with an ogival nose 3 calibres long, and carrying two flat-plate yawing-plane stabilising surfaces (Fig.1). This body was laid out so that the wing planform could be changed systematically without the fuselage line chord extending forward onto the ogive.

(b) Subsequently, for Models 2 and 3, to meet criticisms that the body was unreally long for a tailless layout, it was shortened by 0.75 calibres (Fig.1). This also substantially reduced the pitching inertia of the models (by as much as 20%) which made them nearer the aircraft case (see below).

(c) On Models 4 and 5 the E27/46 fuselage was fairly faithfully reproduced, but without cabin and dorsal fin (Fig.1).

---

[*] In Warren's notation, it can be shown that $H = \frac{1}{2}\left(h_1 + h_2 + \frac{z_{\dot{w}}}{z_w}\right)$.

In all cases the fuselage housed a telemetering set with its transducers and power supply, feeding to aerials set in the trailing edges of the yawing-plane fins, and a number of disturbing rockets with their associated firing circuit and timing clock. Various forms of telemetering set were used (see Table I).

All wings were of RAE 102 section and the same gross planform, a 45° delta with the tips cropped to give a gross taper ratio of 0.125 and gross aspect ratio of 3.11.*

Table I sets out all the models reported here, and gives leading particulars.

The models were boosted to a maximum speed of about 1500 fps, using the separating round technique with a single tandem boost rocket. The model usually got an initial disturbance at separation and the 4 or 5 disturbing rockets were subsequently fired, originally at approximately 1 second intervals, but later at approximately $\frac{1}{2}$ second intervals, in an attempt to bracket the range $0.8 < M < 1.1$.

## 4 Analysis Method

The trajectory was calculated by triangulation from Askania kine theodolite records of the flight; the true air velocity was obtained usually by differencing the trajectory calculations corrected for observed wind component, and for some models this was checked or extended by the use of velocities given by the Reed Doppler instrument, or by integrating a telemetered longitudinal accelerometer. Mach number was calculated from the observed altitude history and observed meteorological conditions.

The method of determining the frequency and damping of an oscillation has been described previously[6]. In addition, in the present instance, when analysing models carrying two longitudinally displaced accelerometers, it is necessary to determine the phase difference and scale ratio between the two oscillations[2]. As in Ref.6, the determination of the phase difference by comparison of the extrapolated times of "Peak 0" (refer to Fig.8 of Ref.6), yielded no useful result, and we were again compelled to resort to computing the phase difference (see para.2). The natural logarithm of the scale ratio is conveniently given as the vertical separation of the two damping curves plotted logarithmically (a typical pair of curves is shown in Fig.8).

## 5 Results

### 5.1 Analysis of frequency data

In Fig.2(a) are plotted the frequency data for all models in the form

$$2\mu \, i_B \, \bar{\omega}_n^2 \;=\; a_1 \, H_m$$

where $H_m$ = manoeuvre margin. The models fall into three groups, according to the C.G. position. Between models 1 and 2 the effect of

---

* The true E27/46 planform is cropped to $\lambda = 0.14$, $A = 3.03$, with some slight rounding of the tip in planform. This is because the present models were originally laid out with nett half wings equal to E27/46 gross half wings. The difference corresponds to our models having a gross span about $1\frac{3}{4}\%$ too large. In all comparisons included in this note the differences are ignored, i.e. aerodynamic centres for example are quoted relative to the same centre line chord position.

0.005 $\bar{c}$ change in C.G. position, (corresponding in the worst case, at subsonic speeds, to a change in $a_1$ $H_m$ of about $\frac{2}{6}$), cannot be separated from the effect of changing the length of the body and scatter, and between models 3 and 4 the effect of a change in body type cannot be detected.

Now the difference between any two curves in Fig.2(a) is due to a constant change in margin $\Delta H_m$, hence from this difference the value of $a_1$ can be deduced. However the value of $a_1$ so deduced, Fig.2(b), when applied to each curve in Fig.2(a), must give a consistent value for the aerodynamic centre position $(H_m + h)$, Fig.2(c). Consistency was achieved as follows:-

(i)   Curves were sketched in through the experimental points in Fig.2(a),

(ii)  Using these curves in pairs, 3 curves for $a_1$ were deduced, and a mean drawn - Fig.2(b),

(iii) Using this mean value for $a_1$ and the experimental values in Fig.2(a), the aerodynamic centre position corresponding to each experimental point was computed - Fig.2(c). Through these, a mean curve was drawn,

(iv)  Using the mean curves from Figs. 2(b) and 2(c) the curves corresponding to the experimental conditions were computed and drawn in Fig.2(a).

After some preliminary trials and adjustments, the curves shown in Fig.2 were arrived at. It should be emphasised again that the curves drawn are self consistent. This set attaches full weight to an experimental point for model 5 at $M = 0.93$ and a point from model 3 at $M = 0.97$ which seem low, at the expense of attaching less weight to three other points, one each from models 1, 2 and 3, at slightly lower Mach numbers. To get all these points to lie on the curves would require some rather rapid oscillations in Figs. 2(b) and 2(c), and bearing in mind the experimental limitations, we did not feel justified in trying to delineate these oscillations from our data, even assuming they exist.

Now although, experimentally, the two points accorded full weight in the above analysis seem well established, the effect of according them less weight seemed worth investigating. Fig.3 shows an analysis in which this has been done. The process was precisely as described above, and again we draw attention to the fact that the set of curves shown is self consistent.

The results of these two analyses for $a_1$ and aerodynamic centre are shown in Fig.5. The difference in $a_1$ at supersonic speeds, about 10%, is a reflection of the reliability of the analysis, and this inevitably gives a change in aerodynamic centre position, in this instance of about 0.04 $\bar{c}$. Shown also in Fig.5(a) are five points calculated from two displaced accelerometers in model 5. The poor agreement with the deduced curves, of two points at about $M = 0.85$ and 1.09, cannot at this stage be adequately explained. Shown also are curves obtained in the RAE High Speed Tunnel[7] and by the RAE Wing Flow Technique (unpublished). These two latter results show good agreement with one another, but they show poor agreement with the present free flight results. The main differences between the conditions of the three tests are shown below.

| Test Method | Model | R at M = 0.9 |
|-------------|-------|--------------|
| Free flight | Complete with body | $6 \times 10^6$ |
| H.S.T. | Half model with body | $1.8 \times 10^6$ |
| Wing Flow | Half model with body | $1 \times 10^6$ |

## 5.2 Analysis of damping data

As described in para.2, we have calculated $m_{\dot{\vartheta}}$ from the expression

$$- m_{\dot{\vartheta}} = 2 \lambda \hat{t} \, i_B - \tfrac{1}{2} a_1 \, i_B.$$

In Fig.4(a) two sets of points are shown; for the large symbols we have used $a_1$ from Fig.2(b), and for the small symbols $a_1$ from Fig.3(b) was used. The difference is within the experimental scatter, except in the range $0.91 < M < 0.95$ where the variation in $a_1$ is greatest. For future manipulations we have adopted $a_1$ from Fig.3(b).

As shown above, it is necessary to correct these values of $m_{\dot{\vartheta}}$ to the same axis position. Writing

$$m_{\dot{\vartheta}} = m_{\dot{\vartheta}_0} + (H - h)^2 \, z_w$$

the adopted variation of $H$ is shown in Fig.4(c). In the range $0.7 < M < 0.97$, $H$ was deduced from the NPL results in Ref.5. Although these have been superseded by later results[8] obtained in a tunnel with slotted walls, they do give measurements for two axis positions, so that $H$ may be deduced, and furthermore the value of $H$ so obtained is in good agreement with that deduced from low speed tests by Moss[9]. At supersonic speeds, $H$ was computed from Ref.4. In common with so many linearised theory results, the value given near $M = 1$ is scarcely plausible, and we have assumed an arbitrary variation as shown in Fig.4(c).

Using Fig.4(c), the measurements (small symbols) in Fig.4(a) were corrected to the axis position used in the latest NPL work[8] namely $0.556 \, c_0 = 0.363 \, \bar{c}$. It is possible to draw a fairly convincing curve through these corrected results, Fig.4(b), from which there are only two large deviations.

In Fig.5(c) the value of $m_{\dot{\vartheta}}$ deduced from the present experiments is compared with Bratt's latest values[8].

## 6 Discussion

### 6.1 The experiment

Comparison of the present results with those obtained on a model with actuated tailplane[6] shows immediately the superiority of the latter method of exciting the oscillation. Firstly, there are more disturbances to analyse (more closely spaced in time and hence Mach number) because the present disturbing rockets are so large that an adequate number cannot be fitted into the model. Also the oscillations are more cleanly excited, because the tailplane moved in much less time than the firing time of the disturbing rocket.

It is doubtful whether even the method of Ref.6 would give an adequate record for a model such as the present, where both $a_1$ and the aerodynamic centre position apparently change rapidly with Mach number. It would be desirable to have a model with a lower drag/weight ratio, so that it passed more slowly through the critical region. In addition the frequency of the oscillation should be high, so that only a short time of oscillation gives an adequate number of cycles to analyse, and this should be obtained with a low inertia rather than a high manoeuvre margin otherwise the determination of $m_\theta^*$ and the aerodynamic centre position suffer.

Instrumentally, the experiment can be done from one model alone provided a measurement of either angle of attack, angular velocity or angular acceleration is available, so that lift curve slope can be determined directly (a longitudinally displaced normal accelerometer as used in model 5 is the equivalent of an angular accelerometer). The development of all these methods is in hand, but further experience is required before any useful comment can be made.

The determination of phase angles seems to be beyond the present telemetering set. This arises apparently from the impossibility of making an adequate simultaneous comparison of two different instruments. We shall have to rely on calculations of phase angles, or methods that do not rely on phase measurement.

### 6.2 The results

The large differences between the present results and those obtained by more entrenched techniques (Fig.5) sends one searching for an explanation.

Bratt's earlier work[5] showed that the damping was very dependent on reduced frequency $\left( \bar{\omega}_n = \omega_n \dfrac{\bar{c}}{V} \right)$ below $\bar{\omega}_n \approx 0.045$. The appropriate values of $\bar{\omega}_n$ for the present models are plotted in Fig.6, and we feel fairly secure from this pitfall.

The experimental results do not show any large body effect, nor does it seem conceivable that the small differences in the gross planform (as mentioned above, to get the wing used by Bratt we would crop the span of our model by 0.30" per wing tip) could be responsible. Our lift curve slopes are, at high subsonic speeds, too high. Assuming the mean $C_L$ of our models to be zero (as was very nearly always true) then Fig.7 shows the range of $C_L$ over which the models oscillated in the present tests, i.e. at M = 1 for example, we have analysed the oscillation during the decay from about $C_L = \pm 0.15$ to about $C_L = \pm 0.02$. Looking at the lift carpets for this model given in Ref.11, this may be an explanation for the difference in $a_1$ between the present tests and those obtained in the High Speed Tunnel, i.e. the lift curves are markedly non linear, $a_1$ ($C_L = \pm 0.05$) being less than $a_1$ ($C_L = \pm 0.2$) especially at M > 0.85.

The aerodynamic centre position (Fig.5(b)) is also affected by the lift curve slope chosen for the analysis of the frequency data. At supersonic speeds, the lift curve slope and aerodynamic centre position obtained in the wing flow experiments give frequency variations that, in Fig.2(a), agree well with those measured on models with an aft C.G. position (models 3 and 4, h = 0.261), but there is a discrepancy that increases as the axis moves forward until for model 1 (h = 0.075) the measured value of $a_1 H_m$ is too low by about 0.2. A similar discrepancy occurs at subsonic speeds. The conclusion is that the experimental data are at variance with the wing flow measurements.

Turning now to the variations of $m_{\dot\theta}$, more serious discrepancies occur (Fig.5(c)). Again, the determination of $m_{\dot\theta}$ from the damping measurements depends on the value of $a_1$. However, assuming the damping measurements to be correct, agreement in $m_{\dot\theta}$ at $M \approx 0.9$ where the biggest discrepancy arises, can be obtained only by assuming a smaller value for $a_1$ than we have used; the value used in the manipulations to give $m_{\dot\theta}$ from the measured damping is greater than that given by the tunnel and wing flow measurements (Fig.5(a)). The effect of using the wing flow measurements of $a_1$, with the present measurements of damping, is to raise the deduced value of $-m_{\dot\theta}$ by about 0.25 between $0.8 < M < 0.9$, and to lower it by about 0.4 in the supersonic region (Fig.5(c)). The final curve is in no better agreement with Bratt's tests. The only plausible change that would bring better agreement between the present and NPL results for $m_{\dot\theta}$ would be a large forward shift of $H\bar{c}$ (Fig.4(c)) so that the subsonic correction for axis position was of the opposite sign. Note again that there is good agreement between the values of $H\bar{c}$ deduced from Refs. 8 and 9.

7.   Conclusions

On the experimental side, it is clear that a much greater number of disturbances per model are required or more identical models. This demands either a much smaller disturbing rocket (so that an adequate number can be housed within a model of reasonable size) or that the disturbance be excited by actuating an elevon (or tailplane). Instrumentally, an all round improvement in the telemetering equipment would give greater confidence in the results.

Aerodynamically the indicated variations with Mach number in lift curve slope, aerodynamic centre position and pitching damping are greater than those obtained by other methods. More weight should be attached to the trends shown by the present experiments than to the absolute magnitudes, but it seems most improbable that all the discrepancy between the present tests and other tests can be due to experimental error.

8   Notation

$a_1$      lift curve slope - per radian

$b$      wing span - feet

$B$      pitching moment of inertia - slugs ft$^2$

$\bar{c}$      mean wing chord - feet

      $= {}^{S}\!/b$

$c_0$      centre line chord - feet

$C_L$      lift coefficient

$C_D$      drag coefficient

$C_m$      pitching moment coefficient

$d$      longitudinal displacement of two accelerometers - feet

$g$      gravity constant - ft/sec$^2$

$h$      position on $\bar{c}$ of centre of gravity

$H$      position on $\bar{c}$ at which $m_{\dot\theta}$ is a maximum

$H_m$      manoeuvre margin stick fixed

$$\approx \ -\left[\frac{dC_m}{dC_L} + h\right]$$

$i_B$      inertia coefficient

$$= \ ^{gB}/_W \ \bar{c}^2$$

$m_q$      pitching moment derivative due to $q$

$m_w$      pitching moment derivative due to $w$

$m_{\dot{w}}$      pitching moment derivative due to $\dot{w}$

$m_{\dot{\vartheta}}$      pitching moment derivative due to $\dot{\vartheta}$

$$= \ m_q + m_{\dot{w}}$$

$m_{\dot{\vartheta}_0}$      maximum value of $m_{\dot{\vartheta}}$, occurs when axis of rotation is at $H$

$M$      Mach number

$n$      normal acceleration - gravity units

$R$      scale ratio between two longitudinally displaced accelerometers

$S$      gross wing area - square feet

$\hat{t}$      aerodynamic time - secs

$$= \frac{\mu \bar{c}}{V} = \frac{W}{g\rho S V}$$

$V$      velocity - ft/sec

$W$      weight of aircraft - lb

$z_w$      normal force derivative due to $w$

$$\approx \ -\tfrac{1}{2} a_1$$

$\alpha$      wing incidence - radians

$\delta$      non dimensional damping

$$= \ \cos^{-1}\left(\frac{\lambda}{\omega_n}\right)$$

$\varphi_d$      phase difference between longitudinally displaced accelerometers

$\lambda$      exponential damping of the longitudinal oscillation

$\mu$      aircraft relative density

$$= \frac{W}{g\rho S \bar{c}}$$

$\nu$      frequency of longitudinal oscillation - cycles/sec

$\rho$      air density - slugs/ft$^3$

$\omega$     circular frequency of longitudinal oscillation - radians/sec

$$= 2\pi\nu$$

$$\omega_n = \left[\omega^2 + \lambda^2\right]^{\frac{1}{2}}$$

$$\bar{\omega}_n = \frac{\omega\bar{c}}{V}$$

---

REFERENCES

| No. | Author | Title, etc. |
|---|---|---|
| 1 | Voepel and Lawrence | Note on a method of determining longitudinal stability data at transonic speeds using ground launched rocket boosted models. RAE Tech Memo No. Aero 124. October 1950. |
| 2 | Voepel | Note on the use of two longitudinally displaced accelerometers in the analysis of the oscillations of free flying bodies. RAE Tech Note No. Aero 2222. February 1953. |
| 3 | Neumark and Thorpe | Theoretical requirements of tunnel experiments for determining stability derivatives in oscillatory longitudinal disturbances. RAE Tech Note No. Aero 2059 (ARC 13667). June 1950. |
| 4 | Warren and Lawrence | A survey of stability and control problems at supersonic speeds with a review of experimental technique. RAE Tech Memo No. Aero 199 (ARC 14250). September 1951. |
| 5 | Bratt, Rayner and Cartwright | Measurements of the direct pitching moment derivatives for a delta wing at high subsonic speeds. ARC 13866. March 1951. |
| 6 | Lawrence and Voepel | The study of stability at transonic speeds by free flying models. Preliminary note on the flight of a model aeroplane with actuated tailplane. RAE Tech Memo No. Aero 293. August 1952. |
| 7 | Pindar and Collingbourne | Pressure plotting and balance measurements in the High Speed Tunnel on a half model of a 90° apex delta wing with fuselage. RAE Report No. Aero 2335 (ARC 12,804). September 1949. |
| 8 | Bratt, Rayner and Townsend | Measurements of the direct pitching moment derivatives for an English Electric transonic wing and a Boulton Paul Delta at transonic speeds. ARC 15206. September 1952. |

REFERENCES (Contd)

| No. | Author | Title, etc. |
|-----|--------|-------------|
| 9 | Moss | Some low speed wind tunnel measurements of damping in pitch for a delta wing.<br>RAE Tech Memorandum No. Aero 123.    November 1950. |
| 10 | Tobak, Reese and Beam | Experimental damping in pitch of $45^\circ$ delta triangular wings.<br>NACA RM No. A50J26 (TIB/2725 = ARC 14438).<br>December 1950. |
| 11 | Evans and Jones | High speed tunnel tests on a $1/12.2$ scale model of a Delta winged aircraft (Boulton Paul E27/46).<br>RAE Report No. Aero 2328 (ARC 12,908).<br>August 1949. |

---

Attached:-      Tables I and II
                Drgs. 28098S – 28103S
                Detachable Abstract Cards

Advance Distribution

PDSR(A)
ADARD(Res)
ADSR(Rec)
TPA3/TIB          150
DARD
DDARD
PIRD(Aircraft)
DMARD(RAF)
NPL (Aero Div)

Director, RAE
DIRAE(A)
RAE Library
GW Dept
Aero (1)
Aero T/A
NAE Library         5
Aero F
   "    H
   "    P
   "    Sup
   "    S
   "    W

## TABLE I

### Details of Models

| | | |
|---|---|---|
| Gross wing area – square feet | S | 2.74 |
| Gross mean chord – feet | $\bar{c}$ | 0.937 |
| Gross aspect ratio | A | 3.11 |
| Gross taper ratio | $\lambda$ | 0.125 |
| Leading edge sweepback | $\Lambda_o$ | 45° |
| Section | RAE 102 | $\tau = 0.10$ |
| Centre line chord – feet | $c_o$ | 1.667 |
| L.E. mean chord $\bar{c}$ aft of L.E. chord $c_o$ – feet | | 0.587 |
| L.E. mean chord $\bar{c}$ as fraction of chord $c_o$ | | 0.353 |

| Model | | 1 | 2 | 3 | 4 | 5 |
|---|---|---|---|---|---|---|
| Weight – lb | W | 37.8 | 41.6 | 42.8 | 30.2 | 38.2 |
| Pitching inertia – slugs ft$^2$ | B | 0.930 | 0.657 | 0.646 | 0.390 | 0.547 |
| $i_B = {}^{gB}/W\bar{c}^2$ | | 0.902 | 0.578 | 0.552 | 0.475 | 0.525 |
| $\mu = {}^{W}/g\rho S\bar{c}$ | | 197 | 216 | 222 | 163 | 203 |
| C.G. on $c_o$ | | 0.462 | 0.465 | 0.499 | 0.500 | 0.395 |
| C.G. on $\bar{c}$ | h | 0.194 | 0.199 | 0.260 | 0.262 | 0.075 |

TABLE II

Body Dimensions of Models 4 and 5

(Dimensions in inches).

| Distance Aft of Nose 'x' | Minor Axis 'y' | Major Axis 'z' |
|---|---|---|
| 2.70 | 3.30 | 5.65 |
| 3.09 | 3.51 | 5.78 |
| 3.67 | 3.79 | 5.92 |
| 4.83 | 4.24 | 6.11 |
| 6.96 | 4.86 | 6.32 |
| 9.09 | 5.26 | 6.39 |
| 10.84 | 5.44 | 6.35 |
| 12.87 | 5.52 | 6.22 |
| 13.36 | 5.52 | 6.18 |
| 15.49 | 5.43 | 5.93 |
| 17.62 | 5.22 | 5.60 |
| 19.75 | 4.92 | 5.20 |
| 21.88 | 4.53 | 4.73 |
|  |  |  |
| 26.14 | 3.70 | 3.70 |
| 31.95 | 1.80 | 1.80 |
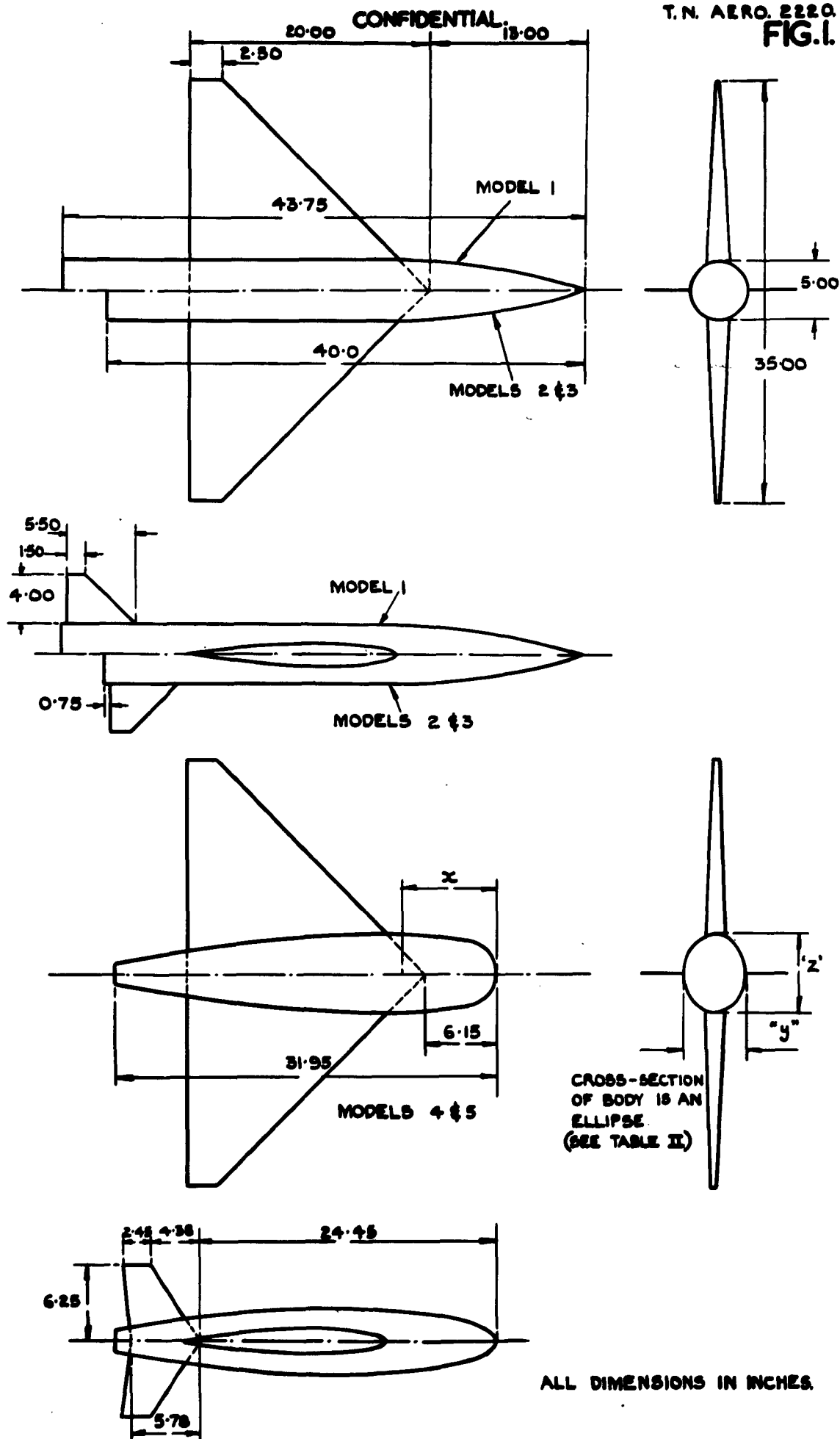
FIG.I.    DETAILS OF MODELS.

| MARK | MODEL | $h_{\bar{c}}$ |
|------|-------|-------|
| × | 1 | 0.194 |
| + | 2 | 0.195 |
| ▼ | 3 | 0.260 |
| ▲ | 4 | 0.262 |
| ● | 5 | 0.075 |



(a) VARIATION OF $a_1 H_m$ WITH M.



(b) VARIATION OF $a_1$ WITH M.



(c) VARIATION OF AERODYNAMIC CENTRE WITH M.

FIG. 2.(a b & c). ANALYSIS OF FREQUENCY DATA
FIRST ATTEMPT.

| MARK | MODEL | $\hbar z$ |
|------|-------|------|
| X | 1 | 0·194 |
| + | 2 | 0·199 |
| ▼ | 3 | 0·260 |
| ▲ | 4 | 0·262 |
| ● | 5 | 0·075 |
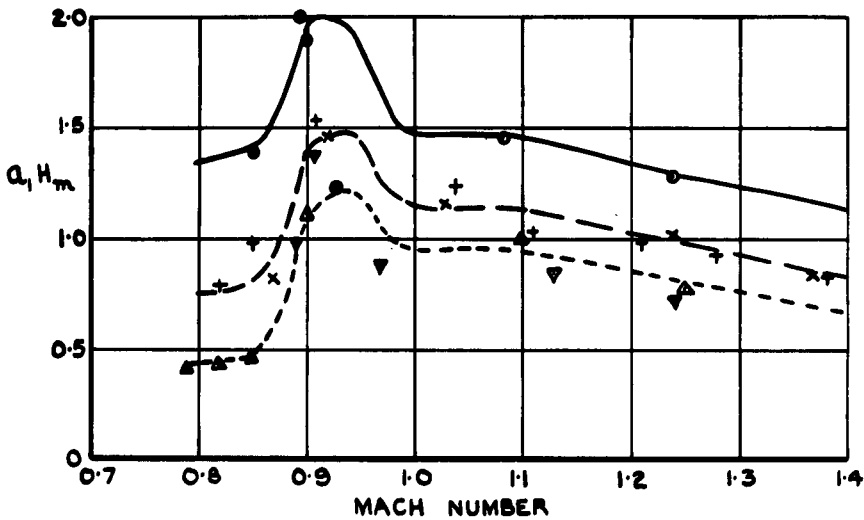
(a) VARIATION OF $a_1 H_m$ WITH M.
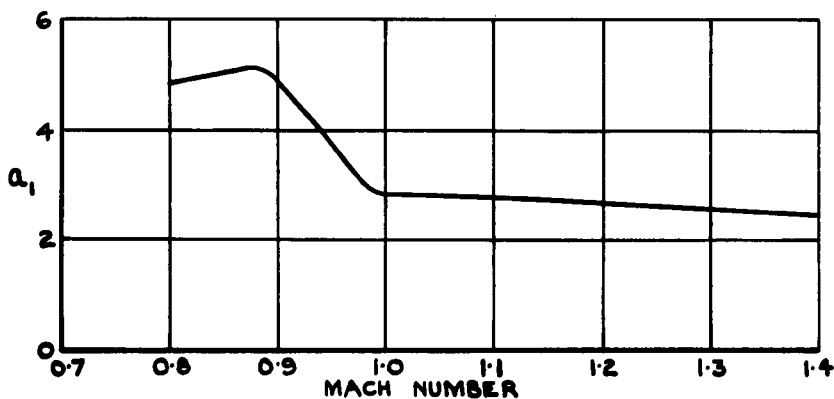
(b) VARIATION OF $a_1$ WITH M.
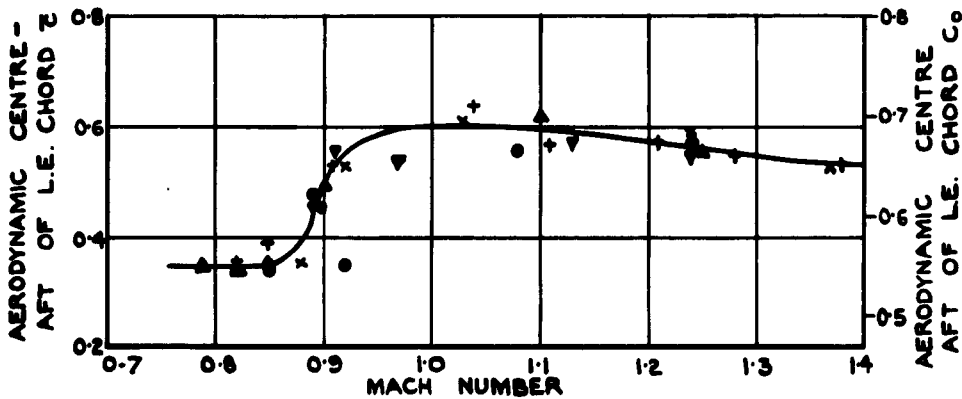
(c) VARIATION OF AERODYNAMIC CENTRE WITH M.

FIG.3(a b & c) ANALYSIS OF FREQUENCY DATA
SECOND ATTEMPT.

X  $a_1$  AS  IN  FIG. 2 (b)
x  $a_1$  AS  IN  FIG. 3 (b)
SYMBOLS  AS  IN  FIG. 2.

$-m_{\dot{\vartheta}}$

1·0

0·5

0

-0·5

-1·0

0·7   0·8   0·9   1·0   1·1   1·2   1·3   1·4

MACH  NUMBER
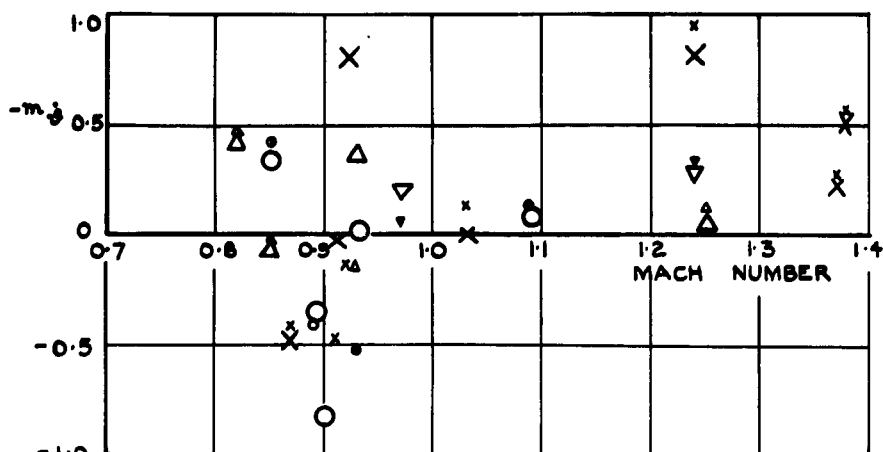
(a)  VARIATION  OF  EXPERIMENTAL  $m_{\dot{\vartheta}_x}$  WITH  M

$-m_{\dot{\vartheta}}$

1·0

0·5

0

-0·5

-1·0

-1·5

0·7   0·8   0·9   1·0   1·1   1·2   1·3   1·4

MACH  NUMBER

CORRECTED TO $\ell = 0.556 C_0 = 0.363 \bar{c}$
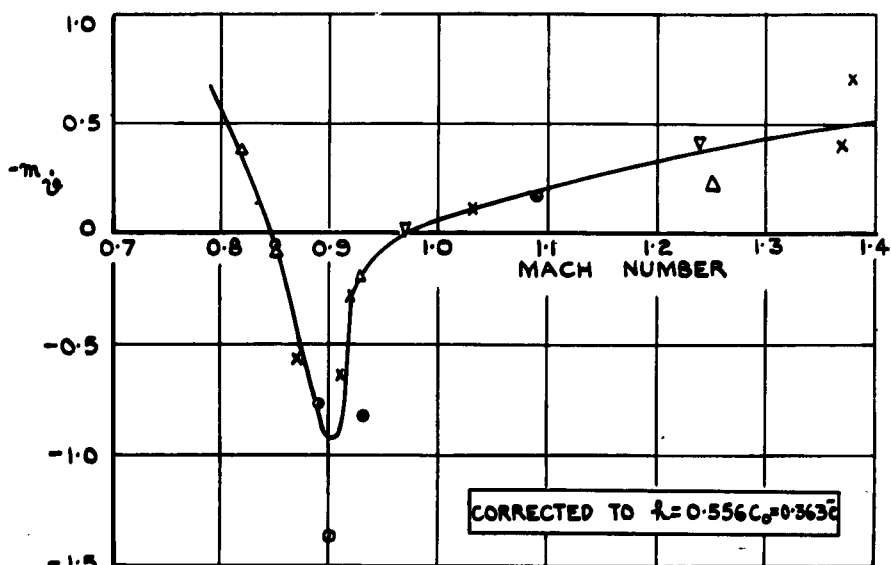
(b)  VARIATION  OF  CORRECTED  $m_{\dot{\vartheta}}$  WITH  M

H

1·0

0·5

0

-0·5

0·7   0·8   0·9   1·0   1·1   1·2   1·3   1·4

MACH  NUMBER

DATA CORRECTED TO
THIS AXIS POSITION

EXP'T REF. 5

ASSUMED

THEORY REF. 4
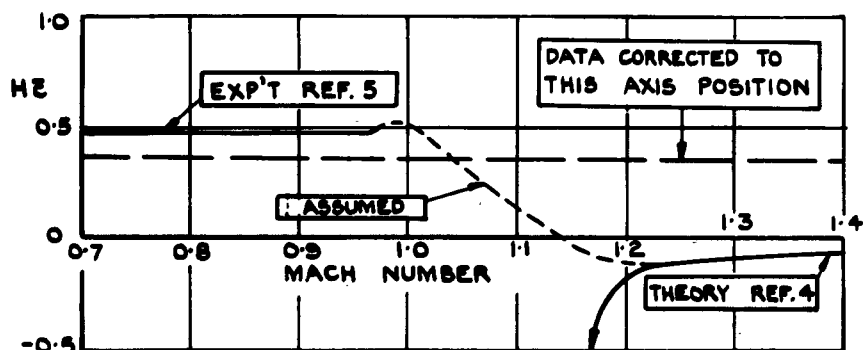
(c)  ASSUMED  VARIATION  OF  H  WITH  M

FIG. 4.(a - c)  ANALYSIS OF DAMPING  DATA.
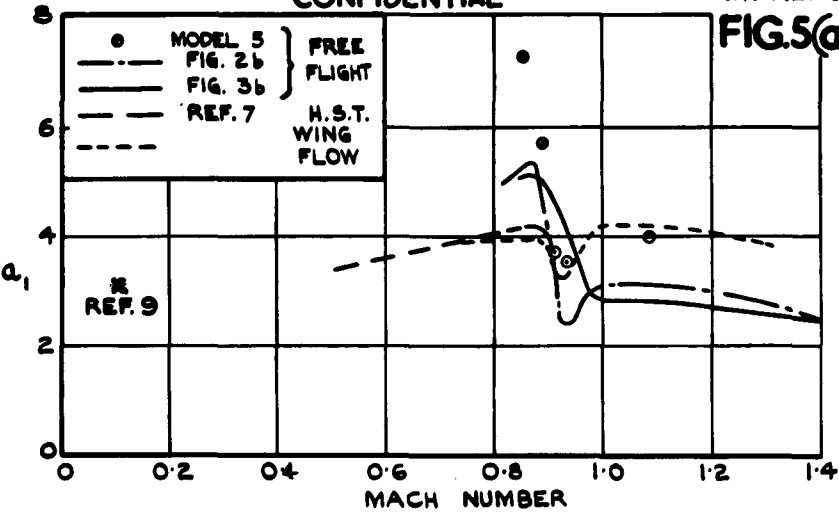
(a) COMPARISON OF $a_1$ MEASUREMENTS.
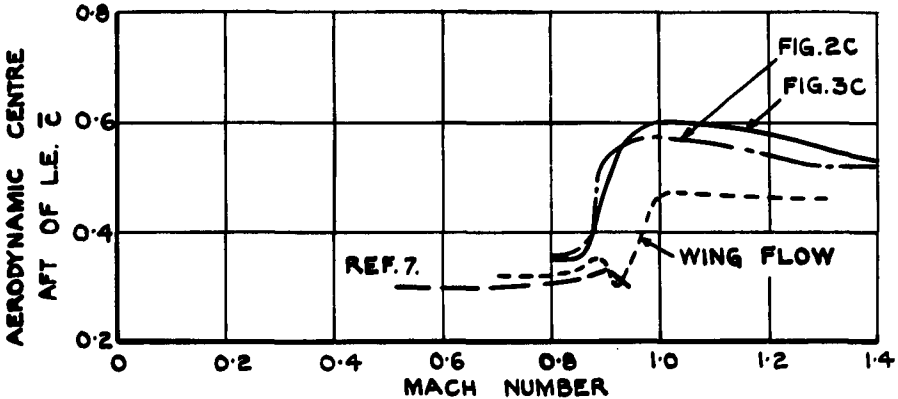


(b) COMPARISON OF AERODYNAMIC CENTRE POSITION.
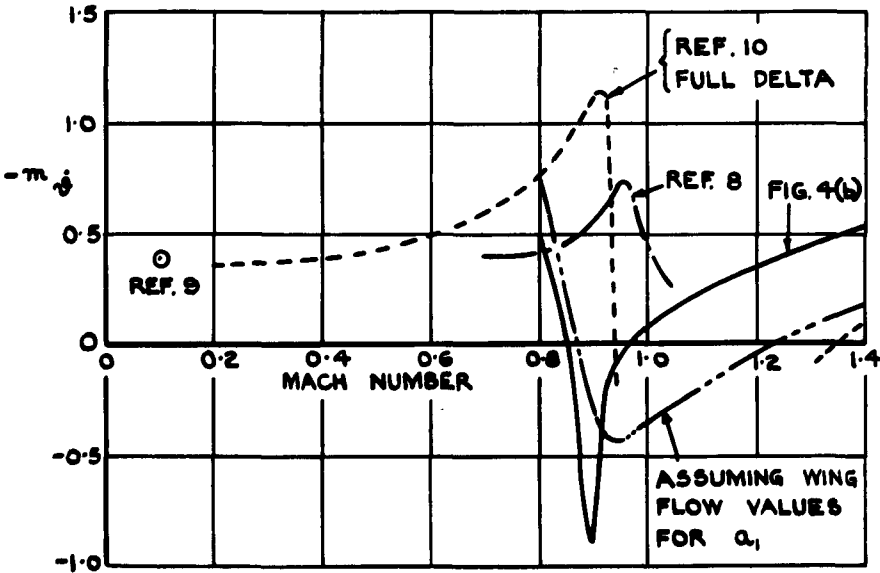


(c) COMPARISON OF $m_{\dot{\vartheta}}$.

FIG.5.(a,b & c) COMPARISON OF RESULTS
FROM DIFFERENT SOURCES.
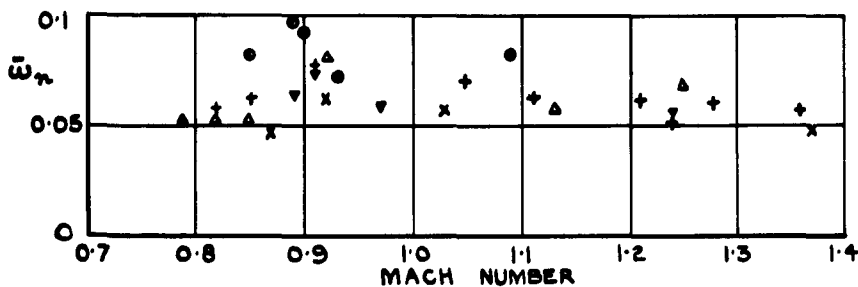
FIG. 6. VARIATION OF REDUCED
FREQUENCY DURING OSCILLATIONS.
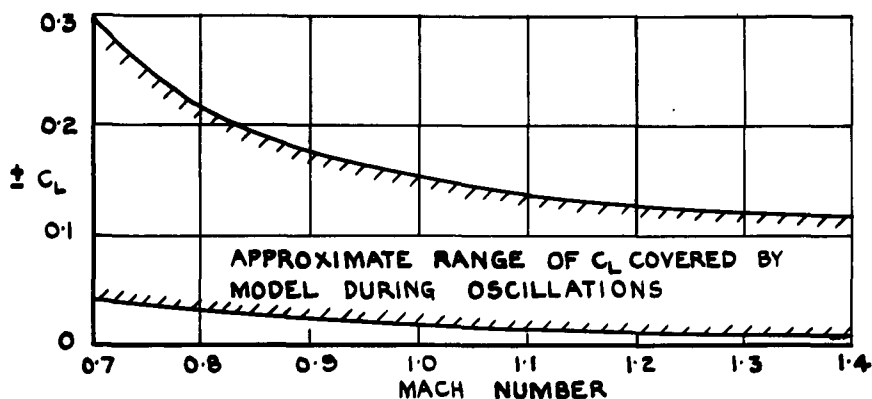


FIG. 7. VARIATION OF LIFT COEFFICIENT
DURING OSCILLATIONS.
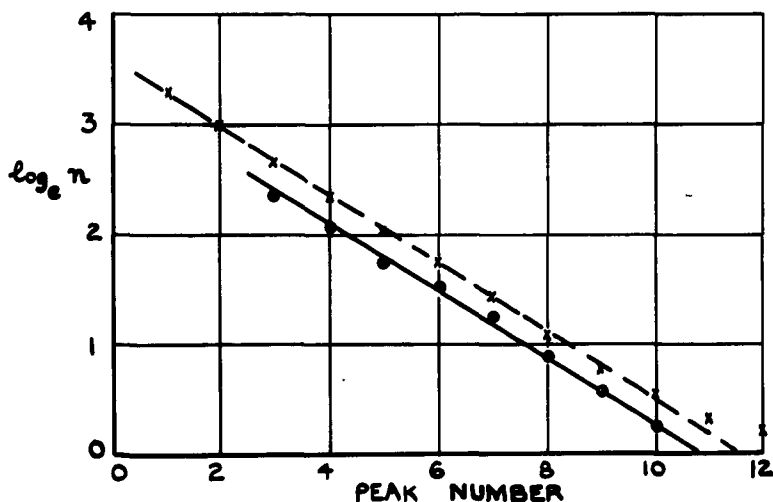


FIG. 8. TYPICAL PLOT SHOWING
DETERMINATION OF DAMPING AND
SCALE RATIO BETWEEN TWO
ACCELEROMETERS.

CONFIDENTIAL

Royal Aircraft Estab. Tech Note No. Aero 2220
1953.1

Lawrence, T. and Harmer, R.

533.652.5.011.35:
533.6.013.422/423:
533.69.043.2:
533.6.013.13:
533.6.013.417(42)E27/46

THE STUDY OF STABILITY AT TRANSONIC SPEEDS BY
FREE FLYING MODELS.
TESTS ON A TAILLESS AEROPLANE WITH 45° DELTA WING
(E27/46)

Five models of a tailless layout having a cropped 45° delta wing (the Boulton Paul Delta layout – E27/46), in which the short period oscillation was excited by small disturbing rockets, were flown in the range $0.8 < M < 1.4$. From measurements of the frequency and damping of the oscillations, the variations with Mach number of lift curve slope, aerodynamic centre position and pitching damping have been deduced, and are compared with measurements from other sources.

1.10.1
1.7.1.2.1
1.8.1.2.3

CONFIDENTIAL

---

CONFIDENTIAL

Royal Aircraft Estab. Tech Note No. Aero 2220
1953.1

Lawrence, T. and Harmer, R.

533.652.5.011.35:
533.6.013.422/423:
533.69.043.2:
533.6.013.13:
533.6.013.417(42)E27/46

THE STUDY OF STABILITY AT TRANSONIC SPEEDS BY
FREE FLYING MODELS.
TESTS ON A TAILLESS AEROPLANE WITH 45° DELTA WING
(E27/46)

Five models of a tailless layout having a cropped 45° delta wing (the Boulton Paul Delta layout – E27/46), in which the short period oscillation was excited by small disturbing rockets, were flown in the range $0.8 < M < 1.4$. From measurements of the frequency and damping of the oscillations, the variations with Mach number of lift curve slope, aerodynamic centre position and pitching damping have been deduced, and are compared with measurements from other sources.

1.10.1
1.7.1.2.1
1.8.1.2.3

CONFIDENTIAL

---

Defense Technical Information Center (DTIC)
8725 John J. Kingman Road, Suit 0944
Fort Belvoir, VA   22060-6218
U.S.A.


AD#:  AD0004780

Date of Search: 14 Apr 2009

Record Summary: AVIA 6/23506
    Title: Tests on tailless aeroplane with 45 deg delta wing (E27/46)
    Availability Open Document, Open Description, Normal Closure before FOI Act: 30 years
    Former reference (Department) Technical Note No Aero 2220
    Held by The National Archives, Kew


This document is now available at the National Archives, Kew, Surrey, United Kingdom.

DTIC has checked the National Archives Catalogue website (http://www.nationalarchives.gov.uk) and found the document is available and releasable to the public.

Access to UK public records is governed by statute, namely the Public Records Act, 1958, and the Public Records Act, 1967.
The document has been released under the 30 year rule.
(The vast majority of records selected for permanent preservation are made available to the public when they are 30 years old. This is commonly referred to as the 30 year rule and was established by the Public Records Act of 1967).


**This document may be treated as <u>UNLIMITED</u>.**